Published in final edited form as:
Biochem J. 2012 December 1; 448(2): 273–283. doi:10.1042/BJ20120730.

Activation of PLC by an endogenous cytokine (GBP) in *Drosophila* S3 cells and its application as a model for studying inositol phosphate signalling through ITPK1

Yixing Zhou[*], **Shilan Wu**[†], **Huanchen Wang**[*], **Yoichi Hayakawa**[‡], **Gary S. Bird**[†], and **Stephen B. Shears**[*,1]

[*]Inositol Signaling Section, Laboratory of Signal Transduction, National Institute of Environmental Health Sciences, National Institutes of Health, Department of Health and Human Services, Research Triangle Park, NC 27709, U.S.A

[†]Calcium Regulation Section, Laboratory of Signal Transduction, National Institute of Environmental Health Sciences, National Institutes of Health, Department of Health and Human Services, Research Triangle Park, NC 27709, U.S.A

[‡]Department of Applied Biological Sciences, Saga University, Honjo-1, Saga 840-8502, Japan

Abstract

Using immortalized [^{3}H]inositol-labelled S3 cells, we demonstrated in the present study that various elements of the inositol phosphate signalling cascade are recruited by a *Drosophila* homologue from a cytokine family of so-called GBPs (growth-blocking peptides). HPLC analysis revealed that dGBP (*Drosophila* GBP) elevated Ins(1,4,5)P_3 levels 9-fold. By using fluorescent Ca^{2+} probes, we determined that dGBP initially mobilized Ca^{2+} from intracellular pools; the ensuing depletion of intracellular Ca^{2+} stores by dGBP subsequently activated a Ca^{2+} entry pathway. The addition of dsRNA (double-stranded RNA) to knock down expression of the *Drosophila* Ins(1,4,5)P_3 receptor almost completely eliminated mobilization of intracellular Ca^{2+} stores by dGBP. Taken together, the results of the present study describe a classical activation of PLC (phospholipase C) by dGBP. The peptide also promoted increases in the levels of other inositol phosphates with signalling credentials: Ins(1,3,4,5)P_4, Ins(1,4,5,6)P_4 and Ins(1,3,4,5,6)P_5. These results greatly expand the regulatory repertoire of the dGBP family, and also characterize S3 cells as a model for studying the regulation of inositol phosphate metabolism and signalling by endogenous cell-surface receptors. We therefore created a cell-line ($S3^{ITPK1}$) in which heterologous expression of human ITPK (inositol tetrakisphosphate kinase) was controlled by an inducible metallothionein promoter. We found that dGBP-stimulated $S3^{ITPK1}$ cells did not synthesize Ins(3,4,5,6)P_4, contradicting a hypothesis that the PLC-coupled phosphotransferase activity of ITPK1 [Ins(1,3,4,5,6)P_5+ Ins(1,3,4)P_3→Ins(3,4,5,6)P_4 + Ins(1,3,4,6)P_4] is driven solely by the laws of mass action [Chamberlain, Qian, Stiles, Cho, Jones, Lesley, Grabau, Shears and Spraggon (2007) J. Biol. Chem. **282**, 28117–28125]. This conclusion represents a fundamental breach in our understanding of ITPK1 signalling.

[1]To whom correspondence should be addressed, shears@niehs.nih.gov.

AUTHOR CONTRIBUTION

Yoichi Hayakawa, Gary Bird and Stephen Shears designed the study. Yoichi Hayakawa synthesized the dGBP peptide. Yixing Zhou, Shilan Wu, Huanchen Wang, Gary Bird and Stephen Shears performed experiments. All authors contributed to writing the paper.

Keywords

calcium; *Drosophila*; inositol phosphate; insect physiology; phospholipase C (PLC)

INTRODUCTION

Stimulus-dependent activation of PLC (phospholipase C) hydrolyses PtdIns(4,5)P_2 to generate two intracellular messengers: diacylglycerol which activates protein kinase C, and Ins(1,4,5)P_3 which binds to specific receptors {IP3R [Ins(1,4,5)P_3 receptor]; itpr in *Drosophila*} that gate intracellular Ca^{2+} stores [1]. This is a ubiquitous signalling response that regulates diverse aspects of cellular biology in almost all animal cell types [1]. As such, it is an intensively studied area of cell biology. Additionally, research into the metabolism of Ins(1,4,5)P_3 has spurred the development of a largely separate signalling industry [2]: the study of an elaborate network of interconnected metabolites, many of which have multiple biological functions (Figure 1 and [2]). Thus the discovery that PLC is activated by an extracellular agonist endows that agent with a large number of new signalling activities.

Drosophila melanogaster is a genetically-tractable eukaryotic model that has proved useful in unraveling the complexities of many aspects of Ca^{2+} signalling [3]. For example, experiments with *Drosophila* mutants have demonstrated that the fly's single *itpr* gene is important for a range of physiological responses [4–6]. Cultured *Drosophila* cells have also been used to study the receptor-dependent activation of Ins(1,4,5)P_3 production and Ca^{2+} mobilization [7–9]. However, the range of opportunities offered by this model organism have not yet been fully exploited for studies into the function and agonist-regulated metabolism of the other inositol phosphate signals (Figure 1). Such studies, which typically rely on analysing cells that have been radiolabelled with [^{3}H]inositol during several days of proliferation [10], are best suited to immortalized cell lines. Such cells have been derived from *Drosophila* [11]. However, there is limited insight into the nature of peptides that act through endogenous receptors to activate PLC in these immortalized cells. The application of these cells to inositol phosphate research has therefore been restricted. To bypass this problem, some groups [7,8] have heterologously expressed exogenous receptors into immortalized *Drosophila* cells. We now describe a more physiologically relevant model that utilizes endogenous receptors: the S3 imaginal-disc cell line [11], in which we show that PLC is activated by a recently discovered insect cytokine, dGBP [*Drosophila* GBP (growth-blocking peptide)] [12].

dGBP is a member of a large family of insect cytokines [13]. These peptides range from 19–30 amino acid residues in length, and are produced upon proteolytic cleavage of longer prepropeptides [13]. The first GBP to be identified was the factor responsible for the reduction in the rate of growth of lepidopteran larvae following their colonization by the larvae of a parasitic wasp, *Costesia kariyai* [14,15]. The endocrinological perturbation that up-regulates GBP synthesis in the host stops it from forming the sclerotized pupal cuticle that would otherwise prevent the parasitic larvae from emerging. The GBP family also regulate morphogenesis, cell proliferation and innate immune responses, for example by stimulating plasmatocyte adhesion and spreading [12,13,16]. However, to date little progress has been made in understanding the molecular mechanisms of action of these cytokines [12]. Recently, the discovery of dGBP has revealed that this peptide acts through c-Jun N-terminal kinase to regulate gene expression [12]. However, in view of the multi-functionality of the GBP family (see above), it has remained probable that these peptides recruit additional signalling pathways. In the present study, we add substantially to dGBP's signalling repertoire by demonstrating its ability to activate multiple facets of the PLC-dependent inositol phosphate/Ca^{2+} cascade.

An increased insight into the molecular actions of insect cytokines such as dGBP is of interest in itself, but the importance of this field of research goes beyond the goal of expanding our understanding of insect physiology [16]. Knowledge of the roles of GBPs in immune responses in pest insects that impair human health or reduce crop yield may lead to the development of improved control programs. There is also considerable evolutionary conservation of innate immunity genes, pathways and effector mechanisms. Research into these defense mechanisms in *Drosophila* may ultimately improve our understanding of human immune responses. Indeed, the identification of the human homologue of the Toll receptor was initially prompted by the discovery that this protein mediates antifungal immune responses in *Drosophila* [17].

Another goal of the present study was to determine whether our discovery that dGBP activates PLC in S3 cells could be exploited to explore the signalling activities of inositol phosphate metabolizing enzymes from higher animals. In pursuit of this idea, we noted that the *Drosophila* genome does not encode a homologue of the mammalian ITPK1 (inositol tetrakisphosphate 1-kinase) [18]. Therefore S3 cells offer a rare example of a model for characterizing any gain-of-function that might arise from the heterologous expression of human ITPK1. For example, the phosphorylation of Ins(1,3,4)P_3 by ITPK1 in mammals (Figure 1A) has been proposed to be the rate-limiting step in the synthesis of Ins(1,3,4,5,6)P_5 and InsP_6 [19]. However, there continue to be differences of opinion [18–21] as to the relative importance of this pathway compared with the alternative ITPK1-independent route to Ins(1,3,4,5,6)P_5 and InsP_6 (Figure 1A). We aimed to address this debate by studying the impact of ITPK1 upon Ins(1,3,4,5,6)P_5 and InsP_6 synthesis in basal and PLC-activated S3 cells. Furthermore, ITPK1 has additional significance to mammalian cell signalling because this enzyme controls the synthesis of Ins(3,4,5,6)P_4 (see Figure 1B), which regulates the conductance of the Cl^- channel/transporter ClC-3 (chloride channel, voltage-sensitive 3) [22]. In this way, ITPK1 helps regulate a number of physiological processes, such as salt and fluid secretion, insulin secretion, and neurotransmission [22–24]. However, it has proved difficult to characterize the mechanism by which Ins(3,4,5,6)P_4 synthesis is accelerated following PLC activation. To explain this phenomenon, we have previously put forward a hypothesis that is based on the laws of mass action [25]. We proposed that an elevated rate of phosphorylation of Ins(1,3,4)P_3 to Ins(1,3,4,6)P_4 by ITPK1 is coupled through an unusual phosphotransferase reaction to an increased rate of dephosphorylation of Ins(1,3,4,5,6)P_5 to Ins(3,4,5,6)P_4 (Figure 1B) [25]. In the present study, we have tested this hypothesis by determining whether PLC-dependent Ins(3,4,5,6)P_4 synthesis could be heterologously introduced into S3 cells by the expression of ITPK1.

MATERIALS AND METHODS Materials

^{3}H-labelled *myo*-inositol and InsP_6 were purchased from PerkinElmer. [^{3}H]Ins(1,4,5)P_3 and [^{3}H]Ins(1,3,4,5)P_4 were purchased from American Radiolabeled Chemicals. [^{3}H]Ins(3,4,5,6)P_4 was prepared as described previously [27]. ^{14}C-labelled inositol phosphates were HPLC-purified from carbachol-stimulated, [^{14}C]inositol-labelled parotid acinar cells. Ins(1,4,6)P_3 was purchased from Cayman Chemicals. Sorbitol dehydrogenase, probenecid and NAD were obtained from Sigma–Aldrich. dGBP was synthesized as described previously [12]. TG (thapsigargin) was purchased from Calbiochem.

Cell culture and stable transfection of S3 cells

Using the EcoRI and XhoI restriction sites, human *ITPK1* cDNA was cloned into a *Drosophila* expression vector, pMT/V5-His (Invitrogen), that includes the metal-inducible metallothionein promoter [26]. Colonies were selected and plasmid DNAs were verified by sequencing. S3 cells (3 ml; 1.5×10^6 cells/well) were seeded in 6-well dishes in Schneider's *Drosophila* medium (Invitrogen) supplemented with 10 % heat-inactivated fetal bovine

serum (Invitrogen), 100 units/ml penicillin and 100 μg/ml streptomycin. After 1 h, cells were transfected (as described in the Effectene Transfection Reagent Handbook; Qiagen) with 1 μg of ITPK1-pMT/V5-His expression vector and 0.05 μg of the resistance plasmid, pCoBlast (Invitrogen). Control cells were transfected with empty vector and the resistance plasmid. Fresh medium was added the following day. At 3 days following transfection, 25 μg/ml blasticidin (Invitrogen) was added to select for stable cell lines, designated S3 and $S3^{ITPK1}$. Colonies were visible in 2–3 weeks, whereupon cells were then transferred to T-25 flasks. Cultures were maintained at 25 °C. Where indicated, the expression of ITPK1 was induced for 2 days with 0.5 mM $CuSO_4$ and the degree of expression was verified by Western blotting analysis [27] of S3 cell lysates, which were prepared in insect cell lysis buffer supplemented with protease inhibitor cocktail (product number 554779; BD Biosciences).

RNA interference

To obtain cDNA fragments of itpr, total RNA was isolated from S3 cells using RNeasy Mini and QIAshredder Kits (Qiagen). Total RNA (1 μg) was reverse transcribed with the following primers: itpr exon 5, forward primer 5′-CCTCAAG-CGTTTGCATCATGC-3′ and reverse primer 5′-CTGTTTT-CCCTTGGGTTTGTCATTTATG-3′; itpr exons 13–18, forward primer 5′-CTGTTCCTGAATCCGGGCATTC-3′ and reverse primer 5′-GCCACAAACAAGCCCTCCTTGC-3′. RT (reverse transcription)–PCR was performed under the following conditions: 55 °C for 1 h and 94 °C for 2 min; then 40 cycles of the following: 94 °C for 15 s, 55 °C for 30 s and 68 °C for 2 min. A final incubation at 72 °C for 10 min was performed.

dsRNA (double-stranded RNA) was prepared by using a MEGAscript RNAi kit (Ambion). For preparing template DNAs, two primers containing a T7 RNA polymerase promoter sequence at their 5′ ends were used. For cDNA fragment of itpr exon 5 (dsRNA-1; 792 bp), the forward primer was 5′-TAA-TACGACTCACTATAGGGGGGCACCTCAATCCAATATG-3′ and the reverse primer was 5′-TAATACGACTCACTATAGG-GTATGGTGGAGTTCATGGTCG-3′. For cDNA fragment of itpr exon 13–18 (dsRNA-2; 744 bp), the forward primer was 5′-TAATACGACTCACTATAGGGCGGAACGCATTCTGTAC-AAC-3′ and the reverse primer was 5′-TAATACGACTCA-CTATAGGGCCGAGGTAGCGCTAACACAAT-3′. For EGFP (enhanced green fluorescent protein) dsRNA (as a control), a PCR product (698 bp) was amplified from a *pEGFP* vector. The forward primer was 5′-TAATACGACTCACTATAGGGAGAG-TGAGCAAGGGCGAGGAG-3′, and the reverse primer was 5′-TAATACGACTCACTATAGGGAGAGATCGCGCTTCTCG-TTGG-3′.

S3 cells were washed three times with serum-free medium and then treated with 20 μg/ml dsRNA for 30–60 min. Fresh medium with 10 % fetal bovine serum was then added and the cells were further incubated at 25 °C for 3 days prior to use. The levels of itpr transcript were determined by RT–PCR (see above) using 2.5 ng of total RNA as a template.

Measurements of inositol phosphates in intact cells

All experiments were performed at 25 °C. Both S3 and $S3^{ITPK1}$ cells (6-well dish; each well contained 5×10^5 cells in 2 ml) were labelled for 4 days with [^{3}H]*myo*-inositol (PerkinElmer; 35 μCi per ml). After 2 days, fresh medium and [^{3}H]*myo*-inositol were added. On day 4, the medium was replaced with a serum-free HBSS (Hepes-buffered salt solution; 120 mM NaCl, 20 mM Hepes, pH 7.4, 5.4 mM KCl, 0.8 mM $MgCl_2$, 10 mM glucose and, unless otherwise stated, 1 mM $CaCl_2$). After a further 1–3 h, LiCl was added to a final concentration of 10 mM for 20 min and then dGBP was added for various times. Assays were quenched by aspiration of medium followed immediately by the addition of 1 ml of

ice-cold 0.6 M perchloric acid/0.02 mM InsP_6. After 20 min on ice, the soluble material was removed and neutralized with 0.4 ml of 1 M potassium bicarbonate/0.04 M EDTA. Samples were stored at 4 °C overnight, centrifuged (10 000 ***g*** for 5 min at 4 °C) to remove insoluble potassium perchlorate, diluted 1:1 with 1 mM EDTA and then analysed using either HPLC or gravity-fed anion-exchange columns [10].

For most HPLC experiments, samples were separated on a 250×4.6 mm Q-100 HPLC column (Thomson Instruments). This is equivalent to the Adsorbosphere SAX columns used in previous studies [28]. The flow-rate was 1 ml/min and the gradient was generated from Buffer A (1 mM EDTA) and Buffer B (1 mM EDTA plus 2 M $NH_4H_2PO_4$, pH 3.35) in the following manner: 0–10 min, 0 % B; 10–110 min, B increased linearly to 63 %. Radioactivity was assessed either with an in-line detector (Radiomatic 500TR) or in 1 ml fractions.

In some experiments, samples were separated on a 125×4.6 mm Partisphere SAX column (Krackeler Scientific) at a flow-rate of 1 ml/min on one of two gradients generated from Buffer A (1 mM EDTA) and Buffer C (1.2 M NaH_2PO_4, pH 4.2). For InsP_3 separation: 0–5 min = 0 % C, 5–76 min C increased linearly to 49 %(InsP_3 eluted at approximately 65 min). For InsP_4 separation: 0–5 min = 0 % C, 5–125 min C increased linearly to 100 %(InsP_4 eluted at approximately 90 min). Fractions of 0.8 ml were collected.

Where necessary, inositol phosphates in HPLC fractions were desalted using Sep-Pak Accell Plus QMA columns (Waters) which were eluted with triethylammonium bicarbonate, and then the samples were freeze-dried [29].

Calcium assays

All procedures were performed at 25 °C. Changes in intracellular Ca^{2+} in populations of Fluo-4-loaded S3 cells were monitored with a fluorometric imaging plate reader (FLIPR^{TETRA} Molecular Devices). Approximately 1×10^5 cells/well were plated in uncoated 96-well plates and incubated for 24 h in 100 μl Schneider's *Drosophila* medium. Then the medium in each well was exchanged for 100 μl HBSS supplemented with 4 μM Fluo-4/AM (Fluo-4 acetoxymethyl ester; Invitrogen) plus 2.5 mM probenecid. After 60 min, cells were washed twice and then incubated in fresh HBSS either in the absence or presence of extracellular Ca^{2+} (1 mM) as indicated. Other reagent additions, indicated in the Figure legends, were made using a remotely controlled robotic 96-tip head. The excitation wavelength for Fluo-4 was 488 nm. Fluorescence emission was selected with a 510–570 nm bandpass filter and monitored simultaneously in all wells with a cooled charge-coupled device camera.

Unless otherwise stated, changes in intracellular Ca^{2+} in individual Fluo-4-loaded S3 cells were monitored in uncoated 48-well plates that were mounted on the stage of a Zeiss LSM 710 confocal microscope equipped with a 10× [0.35 NA (numerical aperture)] objective (approximately 6×10^5 cells/well; 200 μl). The loading of Fluo-4 and analysis of its fluorescence was as described above, except that the incubation volumes/well were 200 μl. Typically, we calculated the average fluorescence intensity of 30–40 single S3 cells for each condition. The data were then expressed as the ratio F/F_0, where F_0 is the average basal fluorescence intensity before cell treatment, and F is the measured fluorescence intensity.

In vitro ITPK1 assays

The Ins(3,4,5,6)P_4 kinase activity of ITPK1 was assayed in 120 μl of buffer containing 2 M Hepes, pH 8.6, 7 mM ATP, 8.7 mM $MgSO_4$ and 0.7 mM EDTA, 5 μg of recombinant ITPK1 ([27]), and 150 μl HPLC fractions containing putative [^{3}H]Ins(3,4,5,6)P_4/

[3H]Ins(1,4,5,6)P_4. Reactions (4 h at 37 °C) were quenched with 0.2 vol. of ice-cold 2 M $HClO_4$ plus 0.1 mg/ml phytate. After 10 min, samples were centrifuged (10 000 ***g*** for 5 min at 4°C), and the supernatants were removed and neutralized with 0.35 vol. of 1 M K_2CO_3 plus 40 mM EDTA. Samples were left at 4 °C overnight before centrifugation and analysis of the supernatant by HPLC. The assay buffer for the phosphotransferase activity of ITPK1 contained 50 mM KCl, 20 mM Hepes (pH 7.0), 6 mM $MgSO_4$, 5 mM ADP, 0.5 mg/ml of BSA, 5 μM [^{3}H]Ins(1,3,4,5,6)P_5, 1 μg of recombinant ITPK1 and, where indicated, 5 μM Ins(1,3,4)P_3. Reactions (30 min) were quenched and neutralized as described above. The Ins(1,3,4)P_3-stimulated dephosphorylation of Ins(1,3,4,5,6)P_5 to Ins(3,4,5,6)P_4 (i.e. the phosphotransferase activity, see Figure 1B and [25]) was recorded using gravity-fed anion-exchange columns [10].

Structural analysis of InsP_3

The treatment of [^{3}H]InsP_3 by periodate oxidation, reduction with sodium borohydride and dephosphorylation with alkaline phosphatase was as described in [10]. The recovery of ^{3}H through each of these procedures was not significantly different from that observed when standards of [^{3}H]Ins(1,4,5)P_3 were processed in parallel. Thus we conclude that none of our samples contained significant quantities of [^{3}H]Ins(4,5,6)P_3 (which would lose the 2-[^{3}H] label during the process [10]). Polyols were resolved by chromatography on a CarboSep CHO-682 HPLC column (Pb form, 300×7.8 mm coupled to a 50×4.6 mm guard column; Transgenomics). Water was used as the eluate, the flow rate was 0.3 ml/min, and the column temperature was 60 °C. The polyol standards that were used to calibrate the column were all obtained from Sigma–Aldrich, except altritol (Tokyo Chemistry Industry) and D-[^{3}H]iditol, which was synthesized by periodate oxidation, reduction and dephosphorylation of [^{3}H]Ins(1,4,5)P_3 [10].

RESULTS

A *Drosophila* cytokine, dGBP, activates PLC in S3 cells

Immortalized *Drosophila* cells have been a relatively untapped resource for studying the regulation of inositol phosphate metabolism by agonist-dependent activation. In the present study we found that the S3 imaginal-disc cell line [11] incorporated radiolabelled [^{3}H]inositol into a variety of inositol phosphates, which were resolved by HPLC (Figure 2A; the elution positions of isomers of InsP_1, InsP_2, InsP_3, InsP_4, InsP_5 and InsP_6 are labelled 1–6). The levels of Ins(1,3,4,5,6)P_5 relative to InsP_6 in S3 cells are relatively low compared with those normally observed in mammalian cells (e.g. Supplementary Figure S1 at http://www.BiochemJ.org/bj/448/bj4480273add.htm). The significance of that comparison is discussed below.

We challenged S3 cells with a newly discovered *Drosophila* cytokine, dGBP [12]. The peptide promoted increases in the levels of InsP_1, InsP_2, InsP_3 and InsP_4 (Figures 2A and 2B) that epitomize PLC activation. These results (Figure 2) provide the first demonstration that dGBP activates various aspects of the PLC-dependent inositol phosphate signalling cascade. The levels of two peaks of InsP_3 were elevated by dGBP (Figures 2B, 3A and 3B). These were identified as Ins(1,3,4)P_3 and Ins(1,4,5)P_3 respectively, on the basis of their co-elution with the standards of these compounds (Supplementary Figures S2A–S2C at http://www.BiochemJ.org/bj/448/bj4480273add.htm), and also by direct structural analysis (Supplementary Figure S2D and Supplementary Table S1 at http://www.BiochemJ.org/bj/448/bj4480273add.htm). Ins(1,3,4,5)P_4 is the metabolic intermediate between Ins(1,4,5)P_3 and Ins(1,3,4)P_3 (Figure 1A). Peak 4a (Figure 2B) was identified as Ins(1,3,4,5)P_4 on the basis of its elution characteristics on two different HPLC systems (Supplementary Figure S3 at http://www.BiochemJ.org/bj/448/bj4480273add.htm). Peak 4b, which we identified as

Ins(1,4,5,6)P_4 (Supplementary Figure S3B), was also elevated following addition of dGBP (Figures 2A and 2B). There is current interest in understanding the mechanisms of the receptor-dependent metabolism of Ins(1,4,5,6)P_4, because of evidence that this particular inositol phosphate is a transcriptional regulator [30,31]. S3 cells may be a useful model for that field of research. dGBP also caused InsP_5 levels to increase by approximately 70 % (control = 1.7±0.18; 2 min stimulation with dGBP = 3.0±0.33; $P < 0.02$).

Note that the height of the dGBP-stimulated Ins(1,4,5)P_3 peak in S3 cells is small compared with the quantities of the Ins(1,4,5)P_3 metabolites, particularly InsP_2 and InsP_1 (Figure 2B). These results suggest a considerable metabolic flux through Ins(1,4,5)P_3, as is typically observed in mammalian cells following agonist-dependent activation of PLC. The degree of the stimulation of PLC by dGBP was also typical of that seen following the activation of endogenous receptors in mammalian cells (Supplementary Figure S1 and [32]). From a dose–response curve for 30 s activation of PLC by dGBP, an EC_{50} value of 0.2 μM was obtained (Figure 2C).

Mobilization of intracellular Ca^{2+} by dGBP

Ins(1,4,5)P_3-dependent Ca^{2+} mobilization is a major consequence of PLC activation [1]. When S3 cells were incubated in medium containing 1 mM Ca^{2+}, the addition of dGBP produced a relatively sustained dose-dependent increase in intracellular Ca^{2+} ; the EC_{50} value was 0.05 μM (Figures 3A and 3B). The EC_{50} value for PLC activation was 4-fold higher (Figure 2C), but differences of this magnitude are not uncommon when comparing dose/response curves data for these two assays (e.g. [33]). Through a phenomenon termed ‘receptor-reserve’ [34], a full Ca^{2+} response may be achieved with less than maximal PLC activation [35].

When S3 cells were incubated in nominally Ca^{2+} -free medium, a rapid increase in intracellular [Ca^{2+}] was still observed after the addition of 0.5 μM dGBP (Figure 3C), but now the Ca^{2+} response was transient (Figure 3C) instead of being sustained (Figure 3A). These results provide a classical demonstration that dGBP initially mobilizes Ca^{2+} from intracellular stores. Nevertheless, the activation of a Ca^{2+} entry pathway following dGBP-dependent store depletion was observed when extracellular Ca^{2+} was restored, resulting in a sustained increase in intracellular [Ca^{2+}] (Figure 3C). Thus dGBP promotes a biphasic Ca^{2+} response that is typically observed following the activation of PLC-coupled receptors: depletion of an intracellular Ca^{2+} store by Ins(1,4,5)P_3, which then drives enhanced Ca^{2+} entry [1,36].

In cells derived from mammals and *Drosophila*, Ca^{2+} signals can also be generated by the addition of TG to inhibit ATP-driven Ca^{2+} uptake by the endoplasmic reticulum [9]; we reproduced these observations in S3 cells (Figures 3C and 3D). In the absence of extracellular Ca^{2+}, the depletion of intracellular Ca^{2+} stores by TG was sufficient to near-completely inhibit the ability of dGBP to mobilize Ca^{2+} (Figures 3E and 3F). It is typical for the Ins(1,4,5)P_3-regulated Ca^{2+} store to overlap with the TG-releasable Ca^{2+} pool [36].

Comparison of the effects of itpr knockdown by dsRNA on dGBP-and TG-induced Ca^{2+} mobilization in S3 cells

To explore further the participation of PLC-dependent Ins(1,4,5)P_3-mediated Ca^{2+} mobilization in the dGBP response, we knocked down expression of the *Drosophila* Ins(1,4,5)P_3 receptor itpr in S3 cells by the addition of dsRNA. Two different dsRNAs gave similar results (results not shown); the effects that were obtained with dsRNA-1 (see the Materials and methods section) are shown in Figure 4.

The degree of expression of itpr was substantially reduced by 3 days of treatment with dsRNA (Figure 4A). There was no effect of the dsRNA upon the degree of dGBP-stimulated PLC activity (Figure 4B). The dsRNA also did not alter the size of the cell's Ca^{2+} stores, since there was no effect upon the degree of Ca^{2+} mobilization that was induced by either TG (Figure 4C) or ionomycin (results not shown). In contrast, itpr knockdown almost completely reduced the ability of dGBP to mobilize intracellular Ca^{2+}, both in the absence (Figure 4D) or presence (Figure 4E) of extracellular Ca^{2+}. These results confirm the involvement of itpr, and hence PLC-dependent Ins(1,4,5)P_3 release, in the dGBP-dependent Ca^{2+} responses described above (and see Figure 3).

The effects of exogenous ITPK1 upon the inositol phosphate profile of unstimulated S3 cells

The heterologous expression of mammalian inositol phosphate kinases in lower eukaryotes has previously proven to be a productive experimental strategy for uncovering new aspects of inositol phosphate metabolism and signalling [37]. The use of an *itpk1*-null cell line as a host for human ITPK1 offers a gain-of-function strategy for studying the roles of this particular kinase. For example, we wished to address some of the uncertainties surrounding the relative importance of ITPK1 in the pathway of Ins(1,3,4,5,6)P_5 and InsP_6 synthesis [18–21].

We generated a stable S3 cell line ($S3^{ITPK1}$) carrying a plasmid encoding the human *ITPK1* gene under the control of the inducible metallothionein promoter. Optimal expression was achieved 48 h post-induction (Figure 5A). The expression of ITPK1 increased InsP_6 levels by approximately 70 %, but Ins(1,3,4,5,6)P_5 levels increased approximately 7-fold (Figures 5B and 5C). There was a corresponding increase in the levels of Ins(1,4,5,6)P_4 (Figure 5C), another metabolite of Ins(1,3,4,5,6)P_5 (Figure 1A). These results demonstrate that ITPK1 can augment the synthesis of these particular inositol phosphates *in vivo*. Nevertheless, the ratio of Ins(1,3,4,5,6)P_5/InsP_6 in S3ITPK1 cells was still substantially below that usually observed in mammalian cells (e.g. Supplementary Figure S1 and [21,32,38]).

Does ITPK1 expression in PLC-activated S3 cells introduce a gain-of-function of Ins(3,4,5,6)P_4 synthesis?

Ins(1,4,5)P_3 is but one of several functionally significant inositol phosphates [2]. Among these, Ins(3,4,5,6)P_4 is a regulator of certain aspects of cell physiology through its control of a Cl^- channel conductance [22–24]. We have proposed that, during PLC activation, an increased rate of phosphorylation of Ins(1,3,4)P_3 to Ins(1,3,4,6)P_4 by ITPK1 is coupled through a phosphotransferase reaction to an increased rate of dephosphorylation of Ins(1,3,4,5,6)P_5 to Ins(3,4,5,6)P_4 (Figure 1B) [25]. Thus one of the goals of the present study was to determine whether PLC-dependent Ins(3,4,5,6)P_4 synthesis would be a gain-of-function following heterologous expression of human ITPK1 in the *itpk1*-null S3 cells.

We first checked whether the expression of ITPK1 might result in an any unexpected modification of PLC activity, which is normally recorded by measuring agonist-dependent accumulation of Ins$P_{(1–4)}$ [10]. That total includes the relatively large quantities of an InsP_3 isomer that accumulated in dGBP-stimulated $S3^{ITPK1}$ cells (peak 3x in Figure 6), but not in wild-type S3 cells (Figures 2A and 2B). Structural analysis (Supplementary Figures S4 and S5 at http://www.BiochemJ.org/bj/448/bj4480273add.htm) identified peak 3x as Ins(1,4,6)P_3. The latter is not a novel isomer; Ins(1,4,6)P_3 has previously been identified in mammalian cells, and its levels also increase somewhat upon receptor activation [32]. However, the high levels of Ins(1,4,6)P_3 that we observed following PLC activation in $S3^{ITPK1}$ cells are unprecedented. There are no known kinases that can synthesize Ins(1,4,6)P_3 from an InsP_2, but either Ins(1,3,4,6)P_4 or Ins(1,4,5,6)P_4 can be precursors

[39,40]. Thus Ins(1,4,6)P_3 was included in our assessment of PLC activity. As explained below, we also deemed that our estimate of dGBP-dependent PLC activity (InsP_n in Figure 7A) should include the synthesis of Ins(1,2,3,4,6)P_5.

In both S3 and S3^{ITPK1} cells, the addition of dGBP stimulated an initial rapid phase of PLC activity that was largely completed within 2 min, after which the levels of inositol phosphates first plateaued and then decreased somewhat (Figure 7A). That transition of the rapid initial phase of PLC activity to a slower secondary rate is a typical manifestation of receptor desensitization, which is important in regulating the duration of an agonist's actions [41]. For example, such desensitization contributes to a largely transient Ins(1,4,5)P_3 response [41]. That was the case in our experiments: a rapid initial 9-fold increase in Ins(1,4,5)P_3 concentration immediately following agonist addition, followed by a slower drop in levels (Figure 7B).

The value of dGBP-stimulated InsP_n was somewhat higher in S3^{ITPK1} cells than in wild-type S3 cells (Figure 7A). However, the presence of Li^+ in these assays does not completely prevent the loss of inositol phosphates by their dephosphorylation to inositol [10]. That loss is probably smaller in S3^{ITPK1} cells, in which a larger proportion of total Ins(1,4,5)P_3 metabolites were 'preserved' for the PLC assay by their conversion into Ins(1,4,5,6)P_4 (Figure 7C), Ins(1,3,4,6)P_4 (Figure 7D and Supplementary Figure S6 at http://www.BiochemJ.org/bj/448/bj4480273add.htm), Ins(1,2,3,4,6)P_5 {presumably produced by off-target IP5K (inositol pentakisphosphate 2-kinase)-mediated phosphorylation of Ins(1,3,4,6)P_4 [42]; Figure 7E} and Ins(1,4,6)P_3 (Figure 7F). Indeed, the levels of those particular metabolites, when added together, near-quantitatively account for the difference in the estimated PLC activity between the two cell types (Figure 7A). Thus we conclude that PLC activity was not greatly modified by ITPK1 expression. There were also no significant differences in the degree of dGBP-mediated Ca^{2+} mobilization between wild-type S3 and S3^{ITPK1} cells (Supplementary Figure S7 at http://www.BiochemJ.org/bj/448/bj4480273add.htm).

We now return to our goal of determining whether, during PLC activation, phosphorylation of Ins(1,3,4)P_3 to Ins(1,3,4,6)P_4 by ITPK1 is coupled through a phosphotransferase reaction to an increased rate of dephosphorylation of Ins(1,3,4,5,6)P_5 to Ins(3,4,5,6)P_4 (Figure 1B and [25]). Ins(1,3,4,6)P_4 was not detected in wild-type S3 cells, but the addition of dGBP to S3^{ITPK1} cells led to a substantial accumulation of Ins(1,3,4,6)P_4 (Figure 7D and Supplementary Figure S6B). These results confirm that the ITPK1 was catalytically active and had access to a substantial supply of Ins(1,3,4)P_3. Furthermore, these results indicate that the flux through the Ins(1,4,5)P_3 kinase/Ins(1,3,4,5)P_4 5-phosphatase pathway (Figure 1A) in dGBP-stimulated S3 cells was much greater than was evident from the low levels of Ins(1,3,4)P_3 (Figure 7G).

If Ins(3,4,5,6)P_4 were to have been produced, it would have co-eluted with its enantiomer, Ins(1,4,5,6)P_4, in peak 4b (Figure 6A). To distinguish between these enantiomers, we incubated aliquots of peak 4b with human ITPK1, which stereoselectively phosphorylates Ins(3,4,5,6)P_4, but not Ins(1,4,5,6)P_4 [43]. We found that there was no phosphorylation of peak 4b by ITPK1 [Figure 8A, closed circles; we estimated that the limits of detection of Ins(3,4,5,6)P_4 in this assay were 1 % of the total peak]. For a positive control, we added [^{3}H]Ins(3,4,5,6)P_4, and found that 80 % of that was phosphorylated by ITPK1 to Ins(1,3,4,5,6)P_5 (Figure 8A, open circles). That is, peak 4b in S3^{ITPK1} was determined to be Ins(1,4,5,6)P_4. It seems unlikely that Ins(3,4,5,6)P_4 was formed in S3ITPK1 cells but then rapidly metabolized; when [^{3}H]Ins(3,4,5,6)P_4 was incubated at 25 °C with S3^{ITPK} cell lysates, its rate of dephosphorylation was <0.03 %/μg/h (results not shown). Indeed, in

mammalian cells Ins(3,4,5,6)P_4 is one of the more metabolically resistant inositol phosphates [23,38].

In separate control experiments, we incubated ITPK1 with aliquots of the corresponding peak 4b from UTP-stimulated BHK (baby hamster kidney) cells (Supplementary Figure S1); virtually all of that peak [equivalent to approximately 10 % of the Ins(1,3,4,5,6)P_5 peak] was found to be Ins(3,4,5,6)P_4 (Figure 7B). This comparison suggests that the mechanism by which ITPK1 synthesizes Ins(3,4,5,6)P_4 in mammalian cells is not reconstituted in S3 cells simply by the expression of ITPK1. That conclusion is inconsistent with our hypothesis that mass-action effects govern the phosphotransferase activity of ITPK1 [25].

One possible consequence of an elevated level of Ins(1,4,6)P_3 in $S3^{ITPK1}$ cells (Figure 7F) could be to inhibit the Ins(1,4,5)P_3 5-phosphatase [44]. Indeed, Ins(1,4,5)P_3 levels were elevated in dGBP-stimulated cells when ITPK1 was expressed (Figure 7B). We therefore next investigated whether Ins(1,4,6)P_3 might also inhibit the phosphotransferase activity of ITPK1, as such an effect was a potential explanation for the absence of Ins(3,4,5,6)P_4 in these cells. We assayed the phosphotransferase activity *in vitro* as previously described [25], that is, from the ability of Ins(1,3,4)P_3 to stimulate ITPK1-catalysed dephosphorylation of Ins(1,3,4,5,6)P_5 into Ins(3,4,5,6)P_4 *in vitro* (Supplementary Figure S8 at http://www.BiochemJ.org/bj/448/bj4480273add.htm). We found that Ins(1,4,6)P_3 did not significantly affect phosphotransferase activity until its concentration was 10-fold greater than that of the Ins(1,3,4,5,6)P_5 substrate (their maximum concentration ratio in intact cells; see below), and then only a 10 % inhibition was observed (Supplementary Figure S8). Thus the presence of Ins(1,4,6)P_3 does not obscure our conclusion that the expression of ITPK1 in S3 cells was insufficient to introduce PLC-coupled Ins(3,4,5,6)P_4 synthesis.

DISCUSSION

A central conclusion in the present study is that PLC is activated by dGBP, a member of a multi-functional family of insect cytokines [13]. The *Drosophila* homologue of the GBP family was identified only quite recently, and it has been shown to stimulate transcription of antimicrobial peptides by activation of c-Jun NH_2-terminal kinase [12]. However, the GBP family is known to regulate other diverse aspects of insect cell physiology, including larval growth, morphogenesis and cell proliferation [12–16]. Therefore it was our goal to search for additional signalling pathways that dGBP might recruit, in order to gain a more complete understanding of the mechanisms that underlie the various actions of these cytokines. Our demonstration that dGBP activates PLC in S3 cells opens up a number of directions for further research into insect physiology. PLC-mediated hydrolysis of PtdIns(4,5)P_2 yields diacylglycerol, which activates protein kinase C, and Ins(1,4,5)P_3, which binds itpr and gates intracellular Ca^{2+} stores [1]. Furthermore, as shown in Figure 7, dGBP also promotes increases in a number of other inositol phosphates, several of which have their own distinct cellular functions [2].

We used several experimental approaches to ascertain that, in S3 cells, dGBP mobilizes Ca^{2+} from intracellular Ins(1,4,5)P_3-releasable stores as a consequence of PLC activation. First, we used HPLC (Figures 2 and 7) and chemical analyses (Supplementary Figure S2) to determine that dGBP promotes the increases in Ins(1,4,5)P_3 and related metabolites that are typical of agonist-dependent stimulation of PLC activity in mammalian cells (e.g. Supplementary Figure S1). Secondly, we used fluorescent Ca^{2+} probes to demonstrate that dGBP promotes the biphasic Ca^{2+} response that is typically observed following the activation of PLC-coupled receptors [1,36]: depletion of intracellular Ca^{2+} stores, which then drives enhanced Ca^{2+} entry (Figure 3). Thirdly, we used dsRNA to knock down itpr

expression, whereupon the ability of dGBP to mobilize intracellular Ca^{2+} stores was almost completely eliminated (Figure 4).

The various elements of the inositol phosphate cascade that are activated by dGBP (Figure 7) have independent functions [2], and so may contribute to the peptide's multi-functionality. The Ins(1,4,5)P_3-mediated mobilization of Ca^{2+} (Figure 3) probably mediates several physiological responses [1]. The dGBP-mediated increases in Ins(1,3,4,5)P_4 levels (Supplementary Figure S3D) may also have some signalling significance [45]. Changes in Ins(1,4,5,6)P_4 levels (Figure 7C) also promise to be important, in the light of evidence that Ins(1,4,5,6)P_4 regulates gene transcription [30,31]. Ins(1,3,4,5,6)P_5 levels in wild-type S3 cells were also elevated by 70 % within 2 min of dGBP addition (Figure 7H and see the Results section). Such a sizable Ins(1,3,4,5,6)P_5 response to PLC activation is not usually observed in mammalian cells (e.g. Supplementary Figure S1H). However, in the murine F9 teratocarcinoma cell line, PLC activation has been associated with large increases in Ins(1,3,4,5,6)P_5 levels, which regulate key aspects of the β-catenin signalling pathway [20]. In F9 cells, Ins(1,3,4,5,6)P_5 synthesis occurs primarily through direct phosphorylation of Ins(1,4,5)P_3 by IPMK (inositol polyphosphate multikinase) [20]. This is also the case in *Drosophila* (Figure 1A and [18]). Thus S3 cells may be of value for further exploring these signalling functions for Ins(1,3,4,5,6)P_5 and their contribution to the physiology of dGBP.

The genetic tractability of *Drosophila* S3 cells is also an advantage when using them to explore the mechanisms of agonist-dependent regulation of the metabolism and functions of the inositol phosphate family. In the present study, we exploited the observation [18] that the *Drosophila* genome is *itpk1*-null, and so we heterologously expressed human ITPK1 in S3 cells in order to gain insight into the signalling functions of that particular kinase. These experiments yielded three significant new conclusions with regards to the actions of ITPK1.

First, we obtained data that are relevant to the ongoing debate concerning the degree to which ITPK1 contributes to Ins(1,3,4,5,6)P_5 synthesis in mammalian cells [18–21,46]. Specifically, we found that the expression of ITPK1 in S3 cells yielded several-fold increases in the steady-state levels of Ins(1,3,4,5,6)P_5 and one of its metabolites, Ins(1,4,5,6)P_4 (Figure 5C). Nevertheless, in both wild-type S3 and $S3^{ITPK1}$ cells, the ratio of Ins(1,3,4,5,6)P_5 to InsP_6 (Figures 5C, 7H and 7I) was relatively low compared with that in mammalian cells (e.g. Supplementary Figure S1 and [21,32,38]). These results suggest that factors other than ITPK1 expression itself contribute to the synthesis of the relatively large quantities of Ins(1,3,4,5,6)P_5 that are typically present in mammalian cells. For example, there is evidence that much of the mammalian cell's Ins(1,3,4,5,6)P_5 resides in a metabolically-resistant pool [47]. The mechanism by which Ins(1,3,4,5,6)P_5 transfers into that pool in mammalian cells may be key to the accumulation of that inositol phosphate at relatively high levels.

Secondly, the sizable accumulation of Ins(1,2,3,4,6)P_5 in PLC-activated $S3^{ITPK1}$ cells (Figure 7E) is also of interest. We attributed that result to the relatively high levels of Ins(1,3,4,6)P_4 (Figure 7D) successfully out-competing the lower levels of Ins(1,3,4,5,6)P_5 (Figure 7H) for phosphorylation by IP5K; such competition has previously been shown *in vitro* [42]. Such a phenomenon could help explain a previously puzzling observation [21] that the InsP_6 pool in rat-1 cells was largely unaffected when Ins(1,3,4,5,6)P_5 synthesis was compromised by knockdown of IPMK expression. An ITPK1-dependent alternative pathway of InsP_6 synthesis in rat-1 in cells could solve that problem: phosphorylation of Ins(1,3,4)P_3 into Ins(1,3,4,6)P_4 (Figure 7D), then into Ins(1,2,3,4,6)P_5 (Figure 7E), which then can be converted into InsP_6 [48].

The third, and arguably the most important, observation to emerge from our studies with ITPK1, was the discovery that the phosphotransferase activity of ITPK1 is not sufficient by itself to recapitulate PLC-dependent synthesis of Ins(3,4,5,6)P_4, an intracellular signal that serves multiple biological roles through its regulation of Cl^- channel activity [22]. Thus our results of the present study counter a previous hypothesis [25] that Ins(3,4,5,6)P_4 levels are solely regulated by the mass-action effects of substrate supply that are exerted upon ITPK1 (see Figure 1B). This outcome was unexpected, because previous structural and metabolic data [25] had indicated that the phosphotransferase activity of human ITPK1 is inherently well-adapted to regulation by mass-action effects *in vitro*. Perhaps the absence of Ins(3,4,5,6)P_4 in PLC-activated $S3^{ITPK1}$ cells (Figure 8A) is because metabolic compartmentalization prevents ITPK1 from accessing Ins(1,3,4,5,6)P_5. It is also possible that there is a yet to be discovered mechanism, not active in S3 cells, by which the phosphotransferase activity of ITPK1 might be activated relative to its kinase activity. A potential mechanism might involve covalent modification of ITPK1, such as by its phosphorylation or acetylation [46]. In any case, the present study indicates that the regulation of the Ins(3,4,5,6)P_4 signalling cascade is more complex than hitherto was appreciated. As the number of physiological responses that are regulated by Ins(3,4,5,6)P_4 increases [22], so the need to unravel these mechanisms becomes more urgent.

In previous work, the heterologous expression in yeast of inositol phosphate kinases of animal and plant origin uncovered new aspects of inositol phosphate metabolism and signalling [37]. However, the use of immortalized *Drosophila* cells as a host offers several advantages over the yeast model, including their more direct relevance to mammalian systems: unlike yeasts, flies have an Ins(1,4,5)P_3-releasable Ca^{2+} pool [4–6]. Genetic manipulation by dsRNA is also cheap and effective in cultured fly cells (e.g. Figure 4). Furthermore, our demonstration in the present study that dGBP stimulates PLC adds value to S3 cells as a resource for further studies into receptor-dependent regulation of inositol phosphate function and metabolism. Our work with ITPK1 offers an example of how that model can usefully be exploited. Finally, we add substantially to the repertoire of the GBP family by demonstrating its ability to activate multiple facets of the PLC-dependent inositol phosphate signalling cascade.

Supplementary Material

Refer to Web version on PubMed Central for supplementary material.

Acknowledgments

We thank Dr X. Qian and Dr J. Mitchell for assistance, and Dr J. Putney and Dr S. Hicks for helpful comments during the writing of the paper.

FUNDING

This work was supported by the Intramural Research Program of the National Institutes of Health/National Institute of Environmental Health Sciences.

Abbreviations used

BHK	baby hamster kidney
dGBP	*Drosophila* growth-blocking peptide
dsRNA	double-stranded RNA
GBP	growth-blocking peptide

HBSS	Hepes-buffered salt solution
IPMK	inositol polyphosphate multikinase
IP5K	inositol pentakisphosphate 2-kinase
ITPK1	inositol tetrakisphosphate 1-kinase
itpr	*Drosophila* Ins(1,4,5)P_3 receptor
PLC	phospholipase C
RT	reverse transcription
TG	thapsigargin

References

1. Berridge MJ. Inositol trisphosphate and calcium signalling mechanisms. Biochim Biophys Acta. 2009; 1793:933–940. [PubMed: 19010359]
2. Hatch AJ, York JD. SnapShot: inositol phosphates. Cell. 2010; 143:1030. [PubMed: 21145466]
3. Chorna T, Hasan G. The genetics of calcium signaling in *Drosophila melanogaster*. Biochim Biophys Acta. 2012; 1820:1269–1282. [PubMed: 22100727]
4. Venkatesh K, Hasan G. Disruption of the IP3 receptor gene of *Drosophila* affects larval metamorphosis and ecdysone release. Curr Biol. 1997; 7:500–509. [PubMed: 9273145]
5. Banerjee S, Lee J, Venkatesh K, Wu CF, Hasan G. Loss of flight and associated neuronal rhythmicity in inositol 1,4,5-trisphosphate receptor mutants of *Drosophila*. J Neurosci. 2004; 24:7869–7878. [PubMed: 15356199]
6. Agrawal N, Padmanabhan N, Hasan G. Inositol 1,4,5- trisphosphate receptor function in *Drosophila* insulin producing cells. PLoS ONE. 2009; 4:e6652. [PubMed: 19680544]
7. Radford JC, Davies SA, Dow JA. Systematic G-protein-coupled receptor analysis in *Drosophila melanogaster* identifies a leucokinin receptor with novel roles. J Biol Chem. 2002; 277:38810–38817. [PubMed: 12163486]
8. Pollock VP, Radford JC, Pyne S, Hasan G, Dow JA, Davies SA. NorpA and itpr mutants reveal roles for phospholipase C and inositol (1,4,5)-trisphosphate receptor in *Drosophila melanogaster* renal function. J Exp Biol. 2003; 206:901–911. [PubMed: 12547945]
9. Roos J, DiGregorio PJ, Yeromin AV, Ohlsen K, Lioudyno M, Zhang S, Safrina O, Kozak JA, Wagner SL, Cahalan MD, et al. STIM1, an essential and conserved component of store-operated Ca^{2+} channel function. J Cell Biol. 2005; 169:435–445. [PubMed: 15866891]
10. Kirk, CJ.; Morris, AJ.; Shears, SB. Inositol phosphate second messengers. In: Siddle, K.; Hutton, JC., editors. Peptide Hormone Action: A Practical Approach. Oxford University Press; New York: 1990. p. 151-184.
11. Schneider I. Cell lines derived from late embryonic stages of *Drosophila melanogaster*. J Embryol Exp Morphol. 1972; 27:353–365. [PubMed: 4625067]
12. Tsuzuki S, Ochiai M, Matsumoto H, Kurata S, Ohnishi A, Hayakawa Y. *Drosophila* growth-blocking peptide-like factor mediates acute immune reactions during infectious and non-infectious stress. Sci Rep. 2012; 2:210. [PubMed: 22355724]
13. Matsumoto H, Tsuzuki S, Date-Ito A, Ohnishi A, Hayakawa Y. Characteristics common to a cytokine family spanning five orders of insects. Insect Biochem Mol Biol. 2012; 42:446–454. [PubMed: 22465148]
14. Hayakawa Y. Juvenile hormone esterase activity repressive factor in the plasma of parasitized insect larvae. J Biol Chem. 1990; 265:10813–10816. [PubMed: 2358440]
15. Hayakawa Y. Structure of a growth-blocking peptide present in parasitized insect hemolymph. J Biol Chem. 1991; 266:7982–7984. [PubMed: 2022627]
16. Jiang H, Vilcinskas A, Kanost MR. Immunity in lepidopteran insects. Adv Exp Med Biol. 2010; 708:181–204. [PubMed: 21528699]

17. Hoffmann JA. The immune response of *Drosophila*. Nature. 2003; 426:33–38. [PubMed: 14603309]
18. Seeds AM, Sandquist JC, Spana EP, York JD. A molecular basis for inositol polyphosphate synthesis in *Drosophila melanogaster*. J Biol Chem. 2004; 279:47222–47232. [PubMed: 15322119]
19. Verbsky JW, Chang SC, Wilson MP, Mochizuki Y, Majerus PW. The pathway for the production of inositol hexakisphosphate in human cells. J Biol Chem. 2005; 280:1911–1920. [PubMed: 15531582]
20. Gao Y, Wang HY. Inositol pentakisphosphate mediates Wnt/β-catenin signaling. J Biol Chem. 2007; 282:26490–26502. [PubMed: 17595165]
21. Fujii M, York JD. A role for rat inositol polyphosphate kinases, rIpk2 and rIpk1, in inositol pentakisphosphate and inositol hexakisphosphate production in Rat-1 cells. J Biol Chem. 2005; 280:1156–1164. [PubMed: 15528195]
22. Mitchell J, Wang X, Zhang G, Gentzsch M, Nelson DJ, Shears SB. An expanded biological repertoire for Ins(3,4,5,6)P_4 through its modulation of ClC-3 function. Curr Biol. 2008; 18:1600–1605. [PubMed: 18951024]
23. Vajanaphanich M, Schultz C, Rudolf MT, Wasserman M, Enyedi P, Craxton A, Shears SB, Tsien RY, Barrett KE, Traynor-Kaplan AE. Long-term uncoupling of chloride secretion from intracellular calcium levels by Ins(3,4,5,6)P_4. Nature. 1994; 371:711–714. [PubMed: 7935818]
24. Renström E, Ivarsson R, Shears SB. Ins(3,4,5,6)P_4 inhibits insulin granule acidification and fusogenic potential. J Biol Chem. 2002; 277:26717–26720. [PubMed: 12055181]
25. Chamberlain PP, Qian X, Stiles AR, Cho J, Jones DH, Lesley SA, Grabau EA, Shears SB, Spraggon G. Integration of inositol phosphate signaling pathways via human ITPK1. J Biol Chem. 2007; 282:28117–28125. [PubMed: 17616525]
26. Bunch TA, Grinblat Y, Goldstein LS. Characterization and use of the *Drosophila* metallothionein promoter in cultured *Drosophila melanogaster* cells. Nucleic Acids Res. 1988; 16:1043–1061. [PubMed: 3125519]
27. Qian X, Mitchell J, Wei SJ, Williams J, Petrovich RM, Shears SB. The Ins(1,3,4)P_3 5/6-kinase/Ins(3,4,5,6)P_4 1-kinase is not a protein kinase. Biochem J. 2005; 389:389–395. [PubMed: 15762844]
28. Glennon MC, Shears SB. Turnover of inositol pentakisphosphates, inositol hexakisphosphate and diphosphoinositol polyphosphates in primary cultured hepatocytes. Biochem J. 1993; 293:583–590. [PubMed: 8343137]
29. Maslanski, JA.; Busa, WB. A sensitive and specific mass assay for myo-inositol and inositol phosphates. In: Irvine, RF., editor. Methods In Inositide Research. Raven Press; New York: 1990. p. 109-122.
30. Odom AR, Stahlberg A, Wente SR, York JD. A role for nuclear inositol 1,4,5-trisphosphate kinase in transcriptional control. Science. 2000; 287:2026–2029. [PubMed: 10720331]
31. Watson PJ, Fairall L, Santos GM, Schwabe JW. Structure of HDAC3 bound to co-repressor and inositol tetraphosphate. Nature. 2012; 481:335–340. [PubMed: 22230954]
32. Barker CJ, Wong NS, Maccallum SM, Hunt PA, Michell RH, Kirk CJ. The interrelationships of the inositol phosphates formed in vasopressin-stimulated WRK-1 rat mammary tumour cells. Biochem J. 1992; 286:469–474. [PubMed: 1530578]
33. White PJ, Webb TE, Boarder MR. Characterization of a Ca^{2+} response to both UTP and ATP at human P2Y11 receptors: evidence for agonist-specific signaling. Mol Pharmacol. 2003; 63:1356–1363. [PubMed: 12761346]
34. Kirk CJ, Creba JA, Downes CP, Michell RH. Hormone-stimulated metabolism of inositol lipids and its relationship to hepatic receptor function. Biochem Soc Trans. 1981; 9:377–379. [PubMed: 6269920]
35. Putney JW Jr, Aub DL, Taylor CW, Merritt JE. Formation and biological action of inositol 1,4,5-trisphosphate. Fed Proc. 1986; 45:2634–2638. [PubMed: 3019783]
36. Parekh AB, Putney JW Jr. Store-operated calcium channels. Physiol Rev. 2005; 85:757–810. [PubMed: 15788710]

37. Seeds AM, Bastidas RJ, York JD. Molecular definition of a novel inositol polyphosphate metabolic pathway initiated by inositol 1,4,5-trisphosphate 3-kinase activity in *Saccharomyces cerevisiae*. J Biol Chem. 2005; 280:27654–27661. [PubMed: 15944147]
38. Oliver KG, Putney JW Jr, Obie JF, Shears SB. The interconversion of inositol 1,3,4,5,6-pentakisphosphate and inositol tetrakisphosphates in AR42J cells. J Biol Chem. 1992; 267:21528–21534. [PubMed: 1328236]
39. Stephens LR, Hawkins PT, Downes CP. An analysis of myo-[^{3}H]inositol trisphosphate found in myo-[^{3}H]inositol prelabelled avian erythrocytes. Biochem J. 1989; 262:727–737. [PubMed: 2590163]
40. Tsujishita Y, Guo S, Stolz LE, York JD, Hurley JH. Specificity determinants in phosphoinositide dephosphorylation: crystal structure of an archetypal inositol polyphosphate 5-phosphatase. Cell. 2001; 105:379–389. [PubMed: 11348594]
41. Menniti FS, Takemura H, Oliver KG, Putney JW Jr. Different modes of regulation for receptors activating phospholipase C in the rat pancreatoma cell line, AR42J. Mol Pharmacol. 1992; 40:727–733. [PubMed: 1719368]
42. Stevenson-Paulik J, Bastidas RJ, Chiou ST, Frye RA, York JD. Generation of phytate-free seeds in *Arabidopsis* through disruption of inositol polyphosphate kinases. Proc Natl Acad Sci USA. 2005; 102:12612–12617. [PubMed: 16107538]
43. Riley AM, Deleu S, Qian X, Mitchell J, Chung SK, Adelt S, Vogel G, Potter BV, Shears SB. On the contribution of stereochemistry to human ITPK1 specificity: Ins(1,4,5,6)P_4 is not a physiologic substrate. FEBS Lett. 2006; 580:324–330. [PubMed: 16376887]
44. Hirata M, Watanabe Y, Yoshida M, Koga T, Ozaki S. Roles for hydroxyl groups of D-myo-inositol 1,4,5-trisphosphate in the recognition by its receptor and metabolic enzymes. J Biol Chem. 1993; 268:19260–19266. [PubMed: 8396130]
45. Miller AT, Chamberlain PP, Cooke MP. Beyond IP_3 : roles for higher order inositol phosphates in immune cell signaling. Cell Cycle. 2008; 7:463–467. [PubMed: 18235237]
46. Zhang C, Majerus PW, Wilson MP. Regulation of inositol 1,3,4-trisphosphate 5/6-kinase (ITPK1) by reversible lysine acetylation. Proc Natl Acad Sci USA. 2012; 109:2290–2295. [PubMed: 22308441]
47. Otto JC, Kelly P, Chiou ST, York JD. Alterations in an inositol phosphate code through synergistic activation of a G protein and inositol phosphate kinases. Proc Natl Acad Sci USA. 2007; 104:15653–15658. [PubMed: 17895383]
48. Stephens LR, Hawkins PT, Stanley AF, Moore T, Poyner DR, Morris PJ, Hanley MR, Kay RR, Irvine RF. Myo-inositol pentakisphosphates. Structure, biological occurrence and phosphorylation to myo-inositol hexakisphosphates. Biochem J. 1991; 275:485–499. [PubMed: 1850990]
49. Saiardi A, Caffrey JJ, Snyder SH, Shears SB. Inositol polyphosphate multikinase (ArgRIII) determines nuclear mRNA export in *Saccharomyces cerevisiae*. FEBS Lett. 2000; 468:28–32. [PubMed: 10683435]
50. Batty IH, Downes CP. The inhibition of phosphoinositide synthesis and muscarinic-receptor-mediated phospholipase C activity by Li^+ as secondary selective consequences of inositol depletion in 1321N1 cells. Biochem J. 1994; 297:529–537. [PubMed: 8110190]

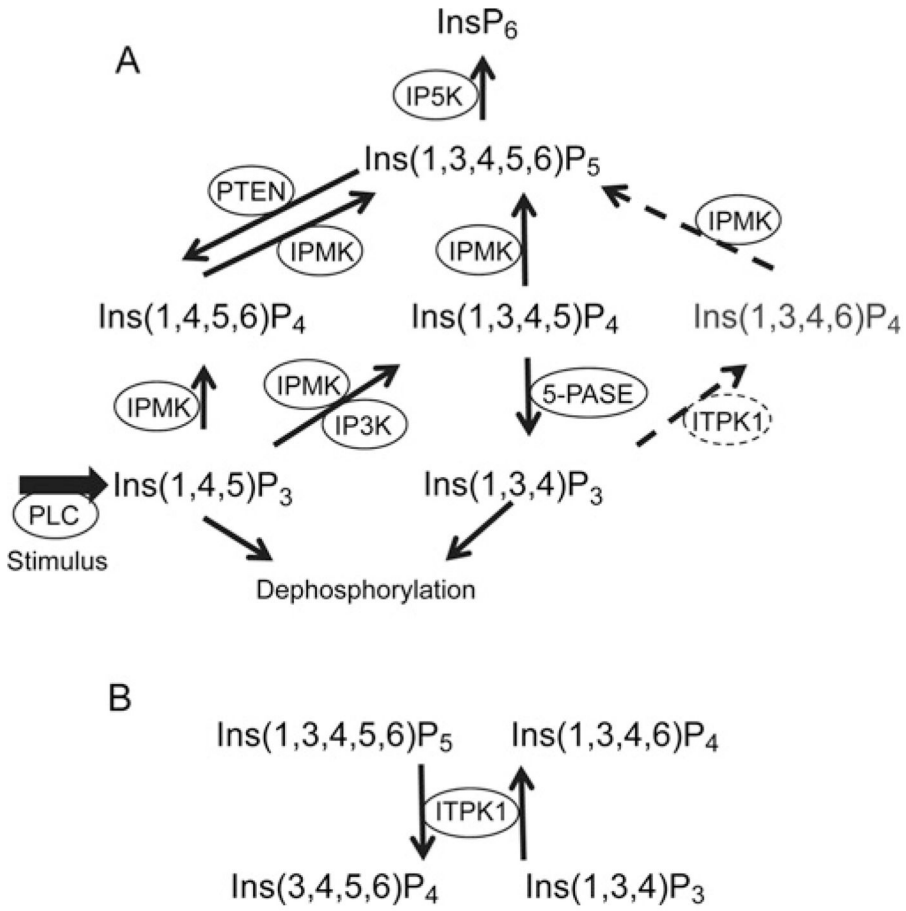

Figure 1. The pathways of inositol phosphate metabolism

(**A**) A depiction of the pathways of inositol phosphate metabolism in animal cells, with a particular emphasis on the multiple contributions from the inositol polyphosphate multikinase, IPMK (reactions involving InsP_1, InsP_2 and the inositol pyrophosphates [2] are omitted for clarity). The reactions depicted by broken arrows are missing from *Drosophila*, which does not express a homologue of ITPK1. IP3K, inositol trisphosphate 3-kinase; 5-PASE, inositol polyphosphate 5-phosphatase; PTEN, phosphatase and tensin homologue deleted on chromosome 10. (**B**) The phosphotransferase activity of ITPK1 (see [25] for details).

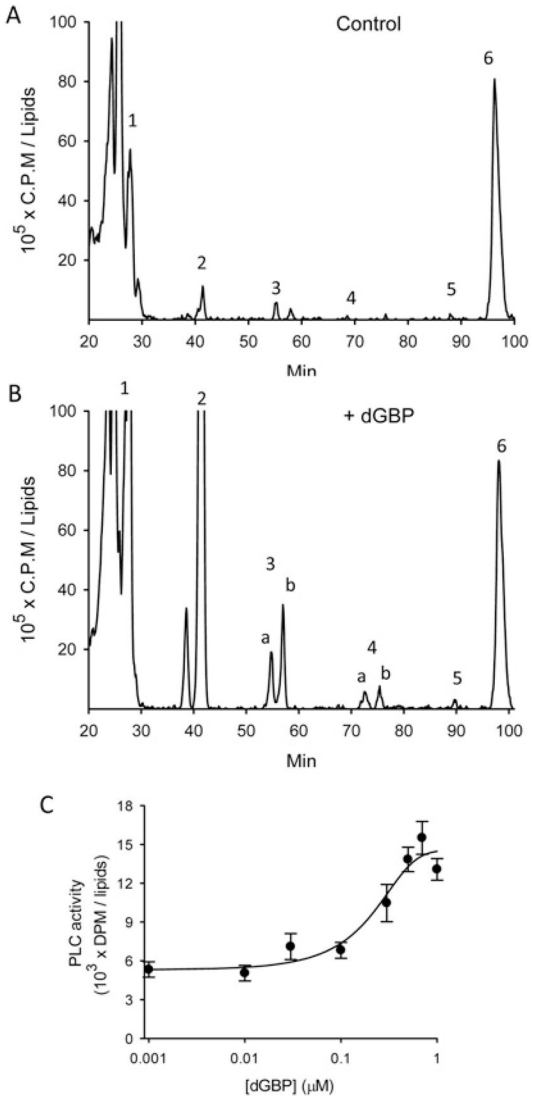

Figure 2. The effect of dGBP upon the inositol phosphate profile of S3 cells

(**A** and **B**) [^{3}H]inositol-labelled S3 cells were incubated with either vehicle (**A**) or 0.5 μM dGBP (**B**) for 2 min and then the samples were quenched, neutralized, separated on a Q100 HPLC column and radioactivity was measured in-line. The numbers that annotate each peak depict the various inositol phosphate species (1, InsP_1 ; 2, InsP_2 etc) as determined with appropriate standards (the present study and [28,49]). Results are from representative experiments (one of four). (**C**) A dose–response relationship between the degree of PLC activation and dGBP concentration (means±S.E.M. from three experiments). The time of stimulation was 0.5 min, and the results were obtained using gravity-fed anion-exchange columns.

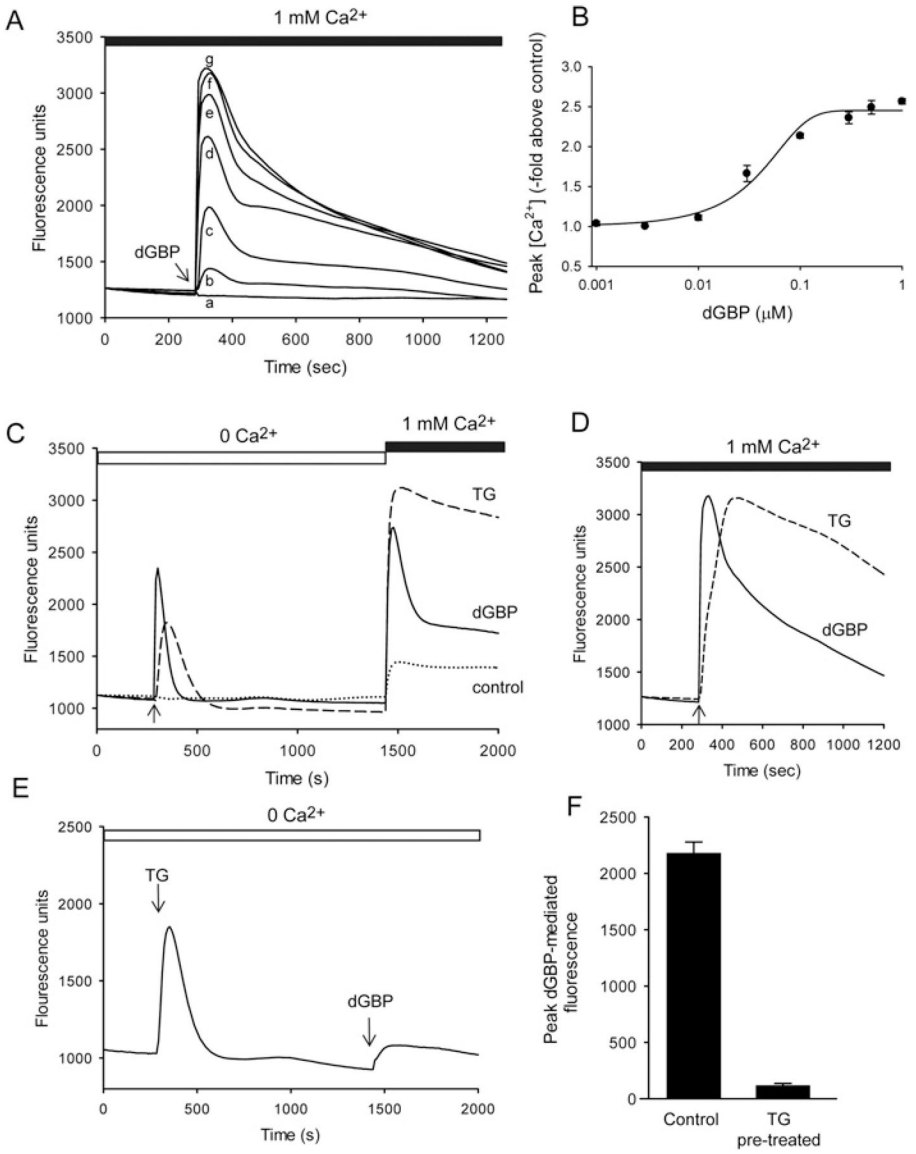

Figure 3. Effects of dGBP peptide and TG on calcium mobilization in S3 cells

Changes in intracellular Ca^{2+} concentration were monitored using Fluo-4 on a fluorometric imaging plate reader ($FLIPR^{TETRA}$). (**A**) Wild-type S3 cells were incubated in medium containing 1 mM Ca^{2+} and were stimulated with the following concentrations of dGBP: 0.003 μM (a), 0.01 μM (b), 0.03 μM (c), 0.1 μM (d), 0.3 μM (e), 0.5 μM (f) or 1 μM (g). Peak [Ca^{2+}] signals were used to generate the dose–response relationship in (**B**). (**C**) Cells were initially incubated in nominally Ca^{2+} -free medium and (where indicated by the arrow) either vehicle (dotted line), 0.5 μM dGBP (continuous line) or 2 μM TG (broken line) were added. Where indicated, 1 mM Ca^{2+} was added to the medium. (**D**) The increase in intracellular [Ca^{2+}] in S3 cells incubated in medium containing 1 mM [Ca^{2+}]; either 0.5 μM dGBP (continuous line) or 2 μM TG (broken line) were added (as indicated by the arrow). (**E**) Cells were incubated in nominally Ca^{2+} -free medium and 2 μM TG and 0.5 μM dGBP were added where indicated. (**F**) S3 cells were incubated in nominally Ca^{2+} -free medium and the peak [Ca^{2+}] signal in response to dGBP was recorded in S3 cells that were pre-treated with either vehicle (left-hand bar) or 2 μM TG (right-hand bar) as in (**E**). The

results are either representative experiments (one of three) or, in (**B**) and (**F**), means±S.E.M. from three experiments.

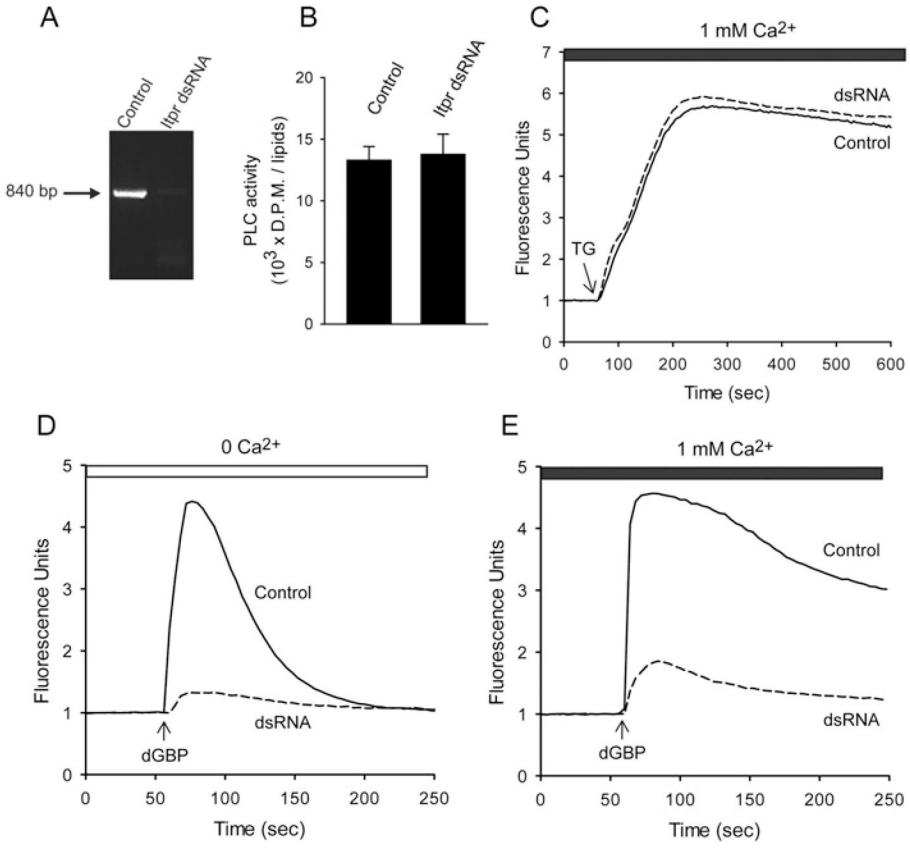

Figure 4. Effects of itpr knockdown by dsRNA on dGBP- and TG-induced calcium mobilization in S3 cells

(**A**) RT–PCR analysis of control or dsRNA-treated cells using gene-specific primers for *itpr*. (**B**) dGBP-stimulated PLC activity of control and dsRNA-treated cells. (**C**–**E**) Changes in intracellular Ca^{2+} were monitored in single Fluo-4-loaded S3 cells seeded in uncoated 48-well plates mounted on the stage of a Zeiss LSM 710 confocal microscope. Cells were incubated either in either nominally Ca^{2+} -free medium (**D**) or medium containing 1 mM Ca^{2+} (**C** and **E**). Either 2 μM TG or 0.5 μM dGBP was added as indicated. The results in (**B**–**E**) are the means of three experiments.

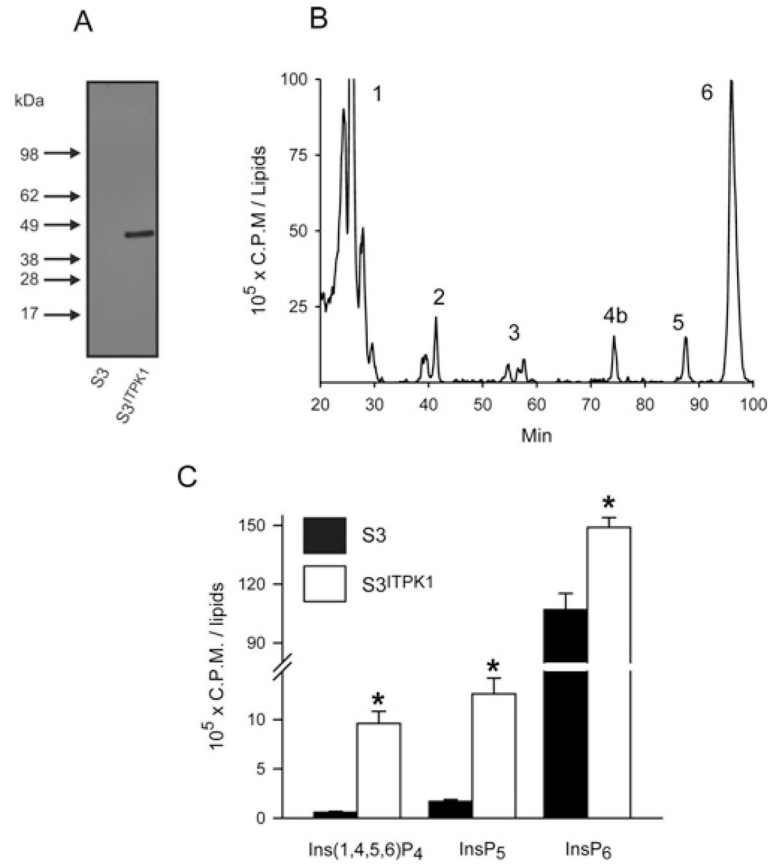

Figure 5. The inositol phosphate profile in S3^{ITPK1} cells

(**A**) Western blotting analysis of ITPK1 in wild-type S3 and S3^{ITPK1} cells. Molecular mass is given on the left-hand side in kDa. (**B**) [^{3}H]inositol-labelled S3^{ITPK1} cells were incubated in serum-free medium for 2 h, and then quenched, neutralized, separated on a Q100 HPLC column, and radioactivity was measured in-line. The numbers that annotate each peak depict the various inositol phosphate species (1, InsP_1 ; 2, InsP_2 etc). (**C**) A comparison of mean levels of Ins(1,4,5,6)P_4, Ins(1,3,4,5,6)P_5 and InsP_6 in wild-type S3 with S3ITPK1 cells (*P < 0.001). Data are either representative experiments (one of four) or means±S.E.M. from four experiments.

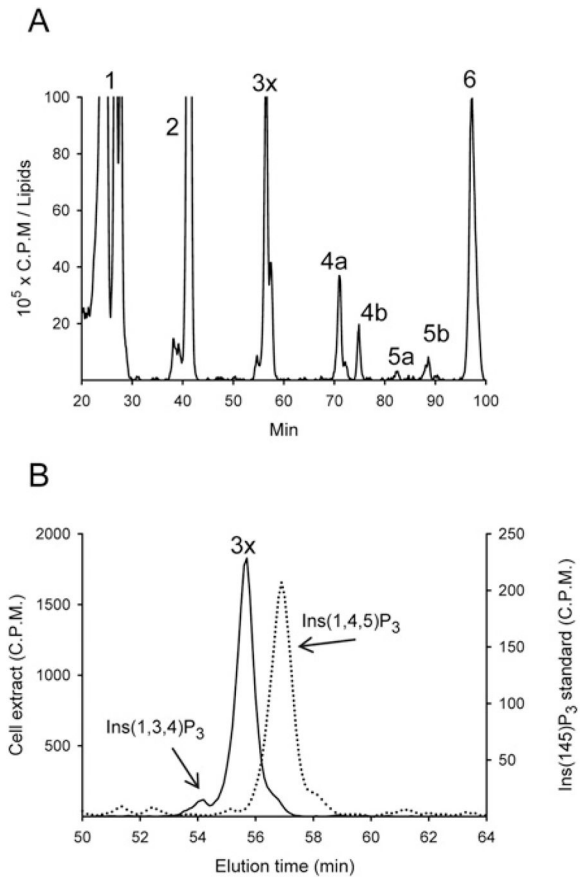

Figure 6. The inositol phosphate profile in dGBP-stimulated S3^{ITPK1} cells

(**A**) [^{3}H]inositol-labelled S3 cells were incubated with 0.5 μM dGBP for 2 min and then the samples were quenched, neutralized and separated on a Q100 HPLC column, and radioactivity was measured in-line. The numbers that annotate each peak depict the various inositol phosphate species (1, InsP_1 ; 2, InsP_2 etc). (**B**) The InsP_3 region of the chromatograph (continuous line) was compared with the elution of a [^{3}H]Ins(1,4,5)P_3 standard from a parallel run (broken line). Peak 3x was identified as Ins(1,4,6)P_3 (see the text for details).

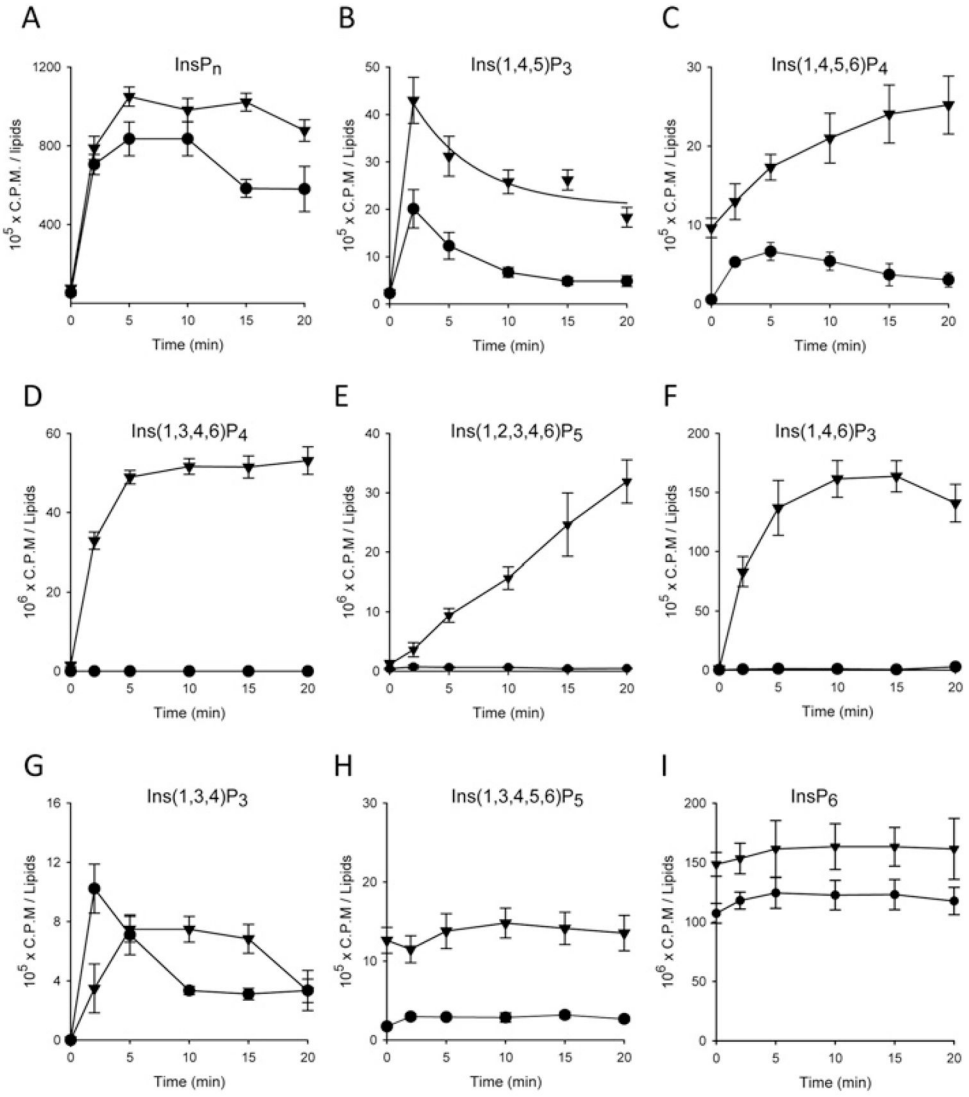

Figure 7. Time course of inositol phosphate metabolism in dGBP-stimulated S3 and S3^{ITPK1} cells

[^{3}H]inositol-labelled wild-type S3 cells (●) or S3^{ITPK1} cells (▼) were incubated with 0.5 μM dGBP for the indicated times and then the samples were quenched, neutralized and separated on a Q100 HPLC column and radioactivity was measured in-line. (**A**) 'InsP_n ' is used as an index of PLC activity and refers to Ins$P_{1–4}$ [41,50] plus Ins(1,2,3,4,6)P_5 (see the text for details). (**B**–**E**) Levels of individual [^{3}H]inositol phosphates. Time-course data for Ins(1,3,4,5)P_4 in wild-type S3 cells are presented in Supplementary Figure S3(D) (at http://www.BiochemJ.org/bj/448/bj4480273add.htm). The results are the means±S.E.M. from four independent experiments. Note that the dGBP-mediated increase in Ins(1,3,4,5,6)P_5 levels in wild-type cells is statistically significant (see the text for details).

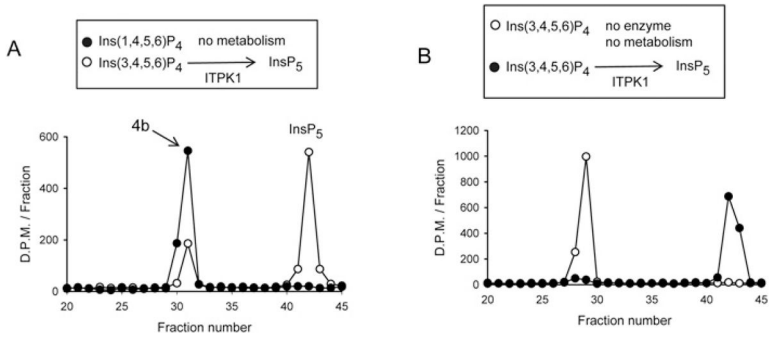

Figure 8. Enzymatic analysis of the proportions of Ins(3,4,5,6)P_4 and Ins(1,4,5,6)P_4 in dGBP-stimulated S3ITPK1 cells and UTP-stimulated BHKITPK1 cells

(**A**) Aliquots of the ^{3}H-labelled peak 4b from S3 cells stimulated with dGBP for 5 min (Figure 2B) (●) or an [^{3}H]Ins(3,4,5,6)P_4 standard (○) were incubated with ITPK1 as described in the Materials and methods section. Samples were quenched, neutralized and separated on a Partisphere SAX column. Note that none of peak 4b was phosphorylated. Similar data were obtained with aliquots of peak 4b isolated from S3 cells stimulated with dGBP for 15 min (results not shown). (**B**) Aliquots of the ^{3}H-labelled peak 4b from BHK^{ITPK1} cells stimulated for 5 min with UTP (Supplementary Figure S1 at http://www.BiochemJ.org/bj/448/bj4480273add.htm) were incubated in either the presence (●) or absence (○) of ITPK1 as described in the Materials and methods section.